

Model for cross-plane thermal conductivity of layered quantum semiconductor structures and application for thermal modeling of GaInAs/AlInAs-based quantum cascade lasers

Khai Q. Le* and Sangin Kim**

School of Electrical and Computer Engineering, Ajou University, Suwon 443-749, South Korea

Received 30 July 2007, revised 21 October 2007, accepted 29 November 2007

Published online 6 February 2008

PACS 42.55.Px, 44.05.+e, 44.10.-i, 73.40.Kp, 73.61.Ey, 73.63.Hs

* Corresponding author: e-mail lqkhai@ajou.ac.kr

** e-mail sangin@ajou.ac.kr

In this paper, a theoretical model for the cross-plane thermal conductivity of layered quantum semiconductor structures is presented. This model is used to evaluate the cross-plane thermal conductivity of the active region in GaInAs/AlInAs-based quantum cascade (QC) lasers. We take into account the temperature dependent thermal conductivity of the layers. By including their interface thermal resistance and scattering processes via the multilayer quantum structure, we predict a decrease by an order of magnitude of the lattice thermal con-

ductivity of the active region in GaInAs/AlInAs-based QC lasers. We computed that the cross-plane thermal conductivity of a InGaAs/AlInAs-based QC laser active region at low temperature from 80 K to 130 K is in the range of 0.5–0.7 W/(m K), whilst the average experimental value obtained by Lops et al. [13] is 0.6 W/(m K). In addition, using the result as input, we present a numerical investigation into the facet temperature profile in this laser during continuous-wave operation using a finite-element method.

© 2008 WILEY-VCH Verlag GmbH & Co. KGaA, Weinheim

1 Introduction Since the first demonstration in 1994 [1], quantum cascade (QC) lasers have been developed as capable sources for mid-infrared to THz radiation. After a decade's effort on the optimization of the active region structures and growth technology, GaInAs/AlInAs-based QC lasers with high output power operating at room temperature (RT) in continuous-wave (CW) as well as pulse mode have been reported [2–4]. However, besides these achievements, the widespread application of these QC lasers still demands significant improvement in the thermal management.

Furthermore, understanding and engineering the thermal properties of QC lasers, especially THz emitters, has become a central issue as we strive for higher-temperature operation. The key limit for RT-CW operation of QC lasers is the large heat dissipation, particularly in the active region. Normally, the active region of a QC laser is about several micrometers in thickness, which contains 25–70 cascaded stages and every stage consists of 15–25 thin layers. However, heat extraction from QC lasers is difficult

due to the high electrical power at laser threshold (typically $P > 4$ W for RT-CW operation [5–7]) and the large thermal resistance from the low thermal conductivity of the QC laser's active region. In order to optimize the thermal performance of QC laser, an accurate theoretical modeling is very necessary. There are several groups making effective thermal analyses, which include Gmachl et al. [8], Spagnolo et al. [9, 10], Zhu et al. [11] and Evans et al. [12]. Recently, Lops et al. [13] measured the facet temperature profiles of GaInAs/AlInAs-based QC lasers operating in CW mode by means of microprobe photoluminescence. These results were used to evaluate the in-plane and cross-plane thermal conductivities of the active region by interpolating from two-dimensional steady-state heat dissipation model based on Fourier's law of heat conduction. However, so far, an accurate theoretical model to predict the cross-plane thermal conductivity of the QC laser active region has not been reported.

In this paper, we present the theoretical calculation model to predict the cross-plane thermal conductivity of

the active region of QC lasers. The model is made based on the previous research results on the total thermal resistivity of layered quantum semiconductor structures along the epitaxy growth direction [14] and the estimated disorder lattice thermal conductivity of semiconductor quantum well structures [15]. The results of numerical simulation carried out for InGaAs/AlInAs-based QC laser show good agreement with recent experimental data obtained by Lops et al. [13]. In addition, using the result as input, we also present a numerical investigation into the facet thermal profile in this laser during CW operation using a finite-element method.

2 Theoretical background The thermal model of QC lasers is generally based upon the steady-state heat dissipation model based on Fourier's law of heat conduction in two dimensions [13]

$$-\nabla \cdot (\mathbf{k} \nabla T) = Q, \quad (1)$$

where \mathbf{k} is the lattice thermal conductivity tensor, Q is the heat generation rate per unit volume, and T is the temperature. For the active region of QC lasers, a large reduction in the thermal conductivity compared with that of bulk materials is demonstrated due to the existence of thousands of interfaces along the epitaxy growth direction [13]. In our thermal simulation of the active region, the in-plane thermal conductivity keeps the bulk value (thickness-weighted average), whilst the cross-plane thermal conductivity simulations are made taking into account the effect of mass interfaces along the epitaxy growth direction. According to the research of Swartz and Pohl [14], the total resistivity along the epitaxy growth direction could be estimated using a Kapitza resistance [thermal boundary resistance (TBR)] as following:

$$r = \frac{a}{a+b} r(a) + \frac{b}{a+b} r(b) + \frac{N}{a+b} \times \text{TBR}, \quad (2)$$

where a and b are, respectively, the total thickness of materials a and b , N is the numbers of interfaces, and $r(a)$ and $r(b)$ are the thermal resistivities of materials a and b with respect to material thickness.

In order to calculate the thickness-dependent thermal resistivity of materials ($r=1/k$), we use the Klemens–Callaway expression [16] for the thermal conductivity under relaxation time approach:

$$k = \frac{k_B}{2\pi^2 v} \left(\frac{k_B T}{\hbar} \right)^3 \frac{\theta_D}{T} \int_0^{\theta_D/T} \tau_c \frac{x^4 e^x}{(e^x - 1)^2} dx, \quad (3)$$

where k_B is the Boltzmann constant, \hbar is the Plank's constant divided by 2π , θ_D is the Debye temperature, $x = \hbar\omega/k_B T$, τ_c is the combined relaxation time, and v is the velocity of sound.

Thermal conductivity calculations and predictions depend on the scattering rate of phonons [17]. When more than one type of scattering process is present, the scattering

rates for all modes are added together and the net relaxation time is given by [18]

$$\tau_c^{-1} = \sum_i \tau_i^{-1}. \quad (4)$$

This expression for the relaxation time must be substituted into Eq. (3) in order to calculate the thermal conductivity as a function of temperature. Limiting our consideration to only three major contributions to the scattering process, we can write the following relation:

$$\tau_c^{-1} = \tau_U^{-1} + \tau_I^{-1} + \tau_B^{-1}, \quad (5)$$

where τ_U , τ_I and τ_B are the relaxation times due to the Umklapp, impurity and boundary scattering processes, respectively.

The relaxation time for the Umklapp process is given by

$$\tau_U^{-1} = A x^2 T^\xi \exp\left(-\frac{B}{T}\right), \quad (6)$$

where A and B are Umklapp parameters, ξ is a number between 2 and 5 and T is the temperature.

The relaxation time due to the boundary scattering can be evaluated from the semiempirical relation [19, 20]

$$\tau_B^{-1} = \frac{v}{W}, \quad (7)$$

where W is some characteristic thickness of the material.

The impurity scattering relaxation time is given by [21]

$$\tau_I^{-1} = \frac{V_0 \omega^4}{4\pi v^3} \Gamma, \quad (8)$$

where

$$\Gamma = \sum_i \Gamma_i \quad (9)$$

is the disorder parameter and V_0 is the volume per atom.

In order to compute the Kapitza resistance, TBR, a diffuse mismatch model (DMM) [14] is used. According to the DMM approach, TBR can be written as

$$\text{TBR} = \left(\frac{1}{2} \sum_j v_{1,j} \Gamma_{1,j} \int_0^{\omega_D} \hbar \omega \frac{dN_{1,j}(\omega, T)}{dT} d\omega \right)^{-1}, \quad (10a)$$

$$N_{1,j}(\omega, T) = \frac{\omega^2}{2\pi^2 v_{1,j}^3 [\exp(\hbar\omega/k_B T) - 1]}, \quad (10b)$$

$$\Gamma_{1,j} = \frac{1}{2} \frac{\sum_j v_{2,j}^{-2}}{\sum_{i,j} v_{i,j}^{-2}}, \quad (10c)$$

$$\omega_D = \frac{k_B \theta_D}{\hbar}, \quad (10d)$$

where $v_{i,j}$ is the phonon velocities, index i ($i = a, b$) stands for different materials and index $j = 1, 2, 3$ stands for longitudinal-acoustic (LA) and two transverse-acoustic (TA) sound velocities and ω_D is the Debye frequency.

Once the Kapitza resistance, TBR, is determined, the average cross-plane thermal conductivity can be obtained from Eqs. (2) and (10a).

3 Results and discussions The theoretical model for the cross-plane thermal conductivity of layered quantum semiconductor structures is employed to compute the cross-plane thermal conductivity of the active region in InGaAs/AlInAs-based QC lasers with various compositions of gallium and aluminum [13]. Also, we first calculated the thermal boundary resistances TBRs of InGaAs/AlInAs systems lattice matched to InP. The material parameters needed for calculation are given in Table 1. The calculated TBR results are depicted in Fig. 1. In the active region of QC lasers, the a to b and b to a interfaces always appear in pairs, so the total thermal boundary resistance could be obtained by counting the total numbers of interfaces and taking the average value of TBR. In the examined QC lasers, the heat-sink temperature is kept at 80 K. At this low temperature TBR increases dramatically, as we can see from Fig. 1. From Eq. (2), the reduced thermal conductivity of InGaAs/AlInAs-based QC laser active region is determined by both bulk and interface effects.

For calculation of the lattice thermal conductivity of materials with respect to their thickness, the Klemens–Callaway expression described in Eq. (3) is used. The best fit to experiment data for 2 μm thick $\text{In}_{0.53}\text{Ga}_{0.47}\text{As}$ [22]

Table 1 Material parameters used in the calculation of thermal boundary resistance (TBR).

material	Debye temperature (K)	wave speed ($\times 10^5$ cm/s)	
		V_L	V_T
$\text{In}_{0.53}\text{Ga}_{0.47}\text{As}$	330	4.25	2.97
$\text{Al}_{0.48}\text{In}_{0.52}\text{As}$	360	4.70	3.01
$\text{In}_{0.64}\text{Ga}_{0.36}\text{As}$	320	4.15	2.90
$\text{Al}_{0.62}\text{In}_{0.38}\text{As}$	385	4.95	3.12

Table 2 Material parameters used in the calculation of the disorder lattice thermal conductivity based on the Klemens–Callaway model.

material	A ($\text{K}^3 \text{s}^{-1}$)	B (K)	velocity of sound ($\times 10^5$ cm/s)	V_0 (\AA^3)	Γ
$\text{In}_{0.53}\text{Ga}_{0.47}\text{As}$	300 ^c	165 ^c	3.30 ^a	25.26 ^a	0.16 ^a
$\text{Al}_{0.48}\text{In}_{0.52}\text{As}$	320 ^c	180 ^c	3.57 ^b	25.25 ^b	0.23 ^b
$\text{In}_{0.64}\text{Ga}_{0.36}\text{As}$	300 ^d	160 ^d	3.22 ^b	25.84 ^b	0.15 ^b
$\text{Al}_{0.62}\text{In}_{0.38}\text{As}$	320 ^d	193 ^d	3.56 ^b	24.54 ^b	0.24 ^b

^a Calculated from Ref. [21].

^b Estimated by using interpolating method.

^c Fitted from experimental data in Refs. [22, 23].

^d The effect of material composition on Umklapp parameters is neglected.

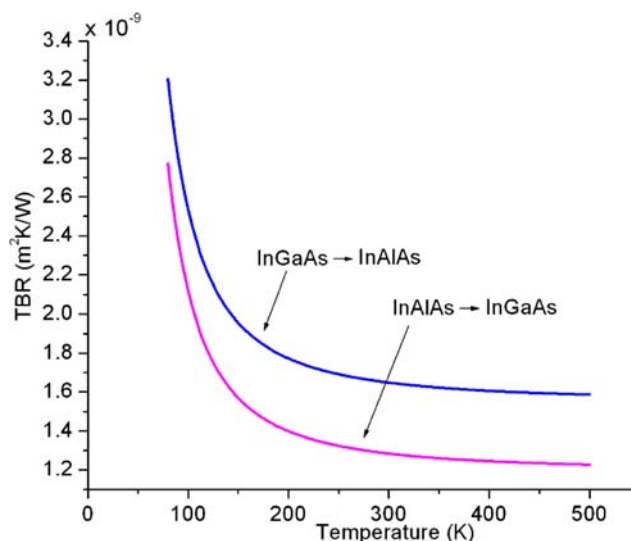


Figure 1 (online colour at: www.pss-a.com) Calculated thermal boundary resistance (TBR) of $\text{In}_{0.53}\text{Ga}_{0.47}\text{As}/\text{Al}_{0.48}\text{Ga}_{0.52}\text{As}$ system lattice matched to InP.

and $\text{Al}_{0.48}\text{In}_{0.52}\text{As}$ [23] can clearly be seen at Fig. 2. The material parameters needed for calculation are listed in Table 2.

Using these results, we then compute the cross-plane thermal conductivity of $\text{In}_{0.53}\text{Ga}_{0.47}\text{As}/\text{Al}_{0.48}\text{Ga}_{0.52}\text{As}$ -based QC laser active region. The calculated results are shown in Fig. 3. In Ref. [13] the authors computed the average cross-plane thermal conductivity of $\text{In}_{0.53}\text{Ga}_{0.47}\text{As}/\text{Al}_{0.48}\text{Ga}_{0.52}\text{As}$ -based QC laser active region by interpolating from experimental data at temperature from 80 K to 130 K at about 0.6 W/m K. Our calculated results were in the range of 0.5–0.7 W/m K. It is clearly seen that these values are consistent with the experimental data. In addition, the results show a large reduction in thermal conductivity of the $\text{In}_{0.53}\text{Ga}_{0.47}\text{As}/\text{Al}_{0.48}\text{Ga}_{0.52}\text{As}$ active region compared to bulk materials [13].

In order to extend the cross-plane thermal conductivity model to QC lasers operating at high temperature, we replicate the cross-plane thermal conductivity of active region in QC laser based on $\text{In}_{0.64}\text{Ga}_{0.36}\text{As}/\text{Al}_{0.62}\text{Ga}_{0.38}\text{As}$ materials [13, 24]. The considered device is composed by a

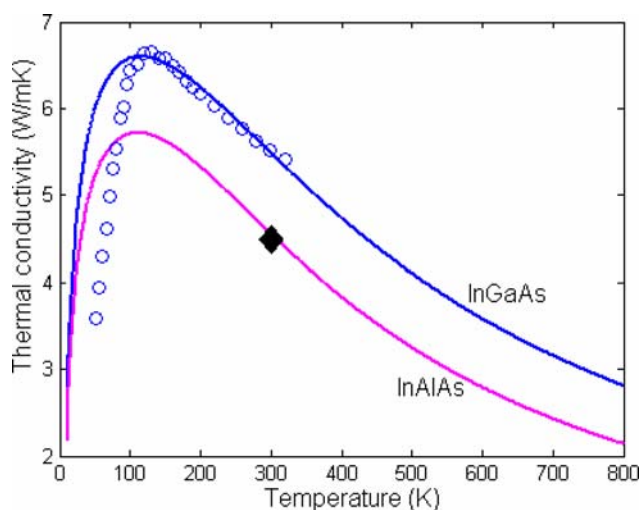


Figure 2 (online colour at: www.pss-a.com) Calculated disorder lattice thermal conductivity of 2 μm thick $\text{In}_{0.53}\text{Ga}_{0.47}\text{As}$ and 2 μm thick $\text{In}_{0.52}\text{Al}_{0.48}\text{As}$ thin films (solid lines). The open circles are experimental data of 2 μm thick $\text{In}_{0.53}\text{Ga}_{0.47}\text{As}$ thin films in Ref. [22] and the diamond symbol is the experimental data of a 2 μm thick $\text{In}_{0.52}\text{Al}_{0.48}\text{As}$ thin film at 300 K in Ref. [23].

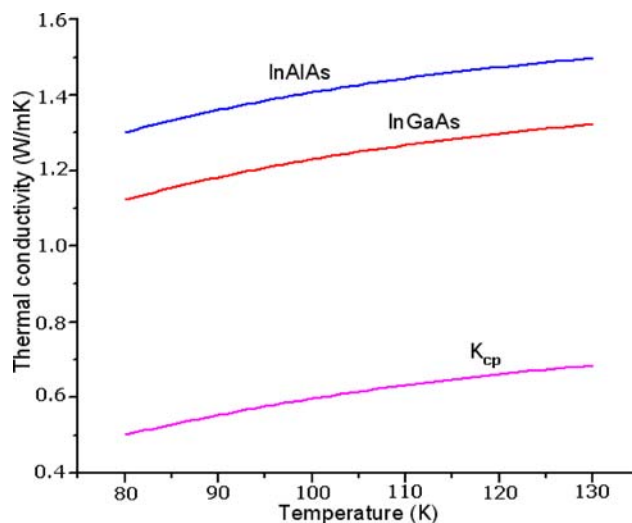


Figure 3 (online colour at: www.pss-a.com) Calculated temperature-dependent thermal conductivity for $\text{In}_{0.52}\text{Al}_{0.48}\text{As}$ and $\text{In}_{0.53}\text{Ga}_{0.47}\text{As}$ in the active region of InGaAs/AlInAs-based QC laser (two top solid lines) and the active region in InGaAs/AlInAs-based QC laser (K_{cp}) along the epitaxy growth direction.

$\sim 1.65 \mu\text{m}$ thick stack of $\text{In}_{0.64}\text{Ga}_{0.36}\text{As}/\text{Al}_{0.62}\text{Ga}_{0.38}\text{As}$ layers, sandwiched between two $\sim 0.3 \mu\text{m}$ thick $\text{In}_{0.53}\text{Ga}_{0.47}\text{As}$ waveguide core layers. Due to the lack of experimental data of thermal conductivity of $\text{In}_{0.64}\text{Ga}_{0.36}\text{As}$ as well as $\text{Al}_{0.62}\text{Ga}_{0.38}\text{As}$ materials, the parameters used for calculation are obtained from the interpolating method and listed in Table 2. The effect of material composition on Umklapp parameters is neglected. Our calculated result of the average cross-plane thermal conductivity of the active region in this laser at temperature from 280 K to 310 K is 1.51 W/m K, while the reported result obtained by these authors is around 2.2 W/m K. It is clearly seen that our

calculated value is still in good agreement with experimental data.

We now pay attention to thermal modeling of $\text{In}_{0.53}\text{Ga}_{0.47}\text{As}/\text{Al}_{0.48}\text{Ga}_{0.52}\text{As}$ -based QC laser. As in recent work [13], thermal modelling based on a two-dimensional steady-state heat dissipation model was carried out. However, in this model, the authors left the cross-plane thermal conductivity of QC laser active region as a fitting parameter. Unlike the previous work, by using the above calculation result of the cross-plane thermal conductivity of the $\text{In}_{0.53}\text{Ga}_{0.47}\text{As}/\text{Al}_{0.48}\text{Ga}_{0.52}\text{As}$ -based QC laser active region as input, we present a numerical investigation on the facet

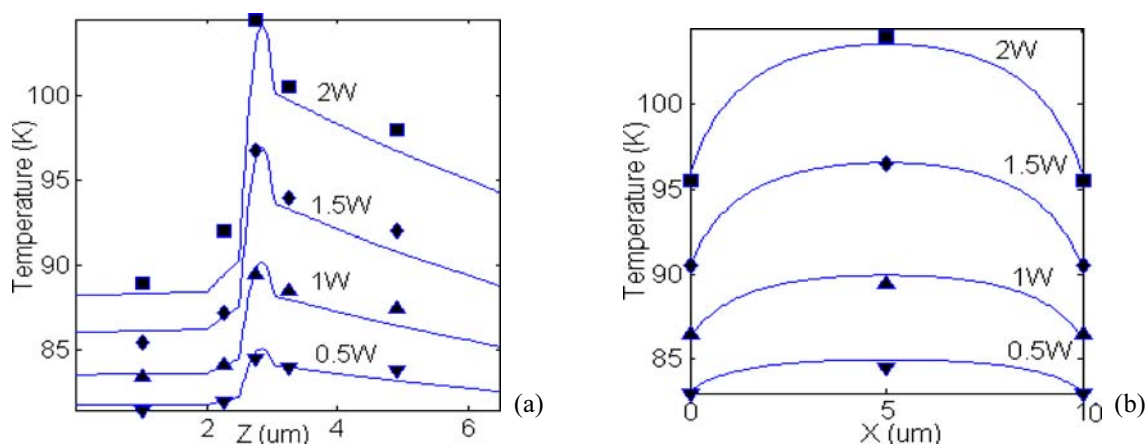


Figure 4 (online colour at: www.pss-a.com) (a) Calculated (solid lines) and referred experimental (symbols) temperature profiles measured along the Z -axis in the center of the device ridge ($X = 0$) for the investigated QC laser driven by CW electrical powers of 0.5 W (▼), 1.0 W (▲), 1.5 W (◆) and 2.0 W (■). (b) Same as (a), measured along the X -axis in the center of the active region ($Z = 0.8 \mu\text{m}$). The heat-sink temperature was kept at $T_{\text{H}} = 80 \text{ K}$.

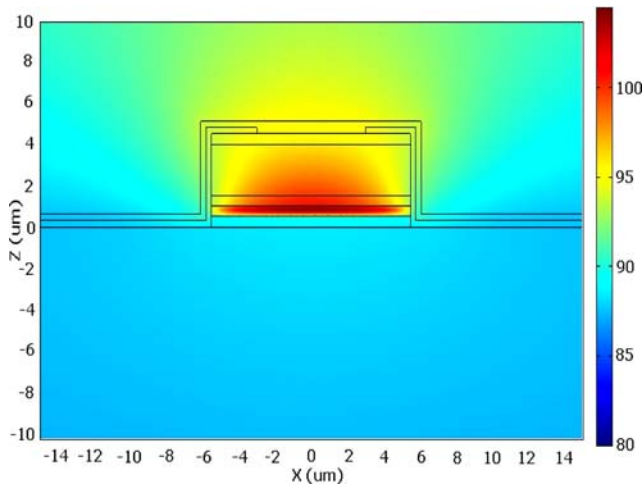


Figure 5 (online colour at: www.pss-a.com) Calculated temperature distribution in the QC laser described in Ref. [13] at $P = 2$ W. The heat-sink temperature was kept at $T_H = 80$ K.

temperature profile in this laser during CW operation using a finite-element method without any fitting parameters and compare the results with experimental data. All the parameters, with the exception of cross-plane thermal conductivity of the active region, needed for simulation are the same as in Ref. [13].

The facet temperature for input electric power P in the range of 0.5–2 W is shown in Fig. 4a and b, whilst Fig. 5 shows the temperature distribution obtained at $P = 2$ W. We assumed most of heat is generated in the active region. From the simulation results, it is seen that temperatures at the edges of the active region are equal and always lower than those are in the center of the device facet. The maximum temperature difference between the active region center and the edges of about 8 K at $P = 2$ W. These simulation results are really consistent with the experimental data.

4 Conclusions We present the theoretical model based on the thermal boundary resistivity (a Kapitza resistance) and scattering processes via multilayer quantum semiconductor structures allowing us to estimate the cross-plane lattice thermal conductivity of layered quantum semiconductor structures. The result of numerical simulation carried out for $\text{In}_{0.53}\text{Ga}_{0.47}\text{As}/\text{Al}_{0.48}\text{Ga}_{0.52}\text{As}$ -based QC laser active region shows good agreement with experimental data. Using this result combined with known parameters as inputs, we have enough parameters needed to perform

the thermal modeling of $\text{In}_{0.53}\text{Ga}_{0.47}\text{As}/\text{Al}_{0.48}\text{Ga}_{0.52}\text{As}$ -based QC lasers. In addition, the presented calculation procedure is applicable in the most usual $\text{InGaAs}/\text{AlInAs}$ -based QC lasers operating at temperatures up to room temperature and is very useful for their thermal designs.

References

- [1] J. Faist, F. Capasso, D. L. Sivco, A. L. Hutchinson, and A. Y. Cho, *Science* **64**, 553 (1994).
- [2] J. S. Yu, A. Evans, J. David, L. Doris, S. Slivken, and M. Razeghi, *IEEE Photon. Technol. Lett.* **16**, 747 (2004).
- [3] J. Faist, D. Hofstetter, M. Beck, T. Aellen, M. Rochat, and S. Blaser, *IEEE J. Quantum Electron.* **38**, 533 (2002).
- [4] A. Friedrich, G. Scarpa, G. Boehm, and M. C. Amann, *Electron. Lett.* **40**, 1416 (2004).
- [5] A. Evans, J. S. Yu, J. David, L. Doris, K. Mi, S. Slivken, and M. Razeghi, *Appl. Phys. Lett.* **84**, 314 (2004).
- [6] S. Blaser, D. A. Yarekha, L. Hvozdar, Y. Bonetti, A. Muller, M. Giovannini, and J. Faist, *Appl. Phys. Lett.* **86**, 041109 (2005).
- [7] J. S. Yu, S. Slivken, S. R. Darvish, A. Evans, B. Gokden, and M. Razeghi, *Appl. Phys. Lett.* **87**, 041104 (2005).
- [8] C. Gmachl et al., *IEEE Photonics Technol. Lett.* **11**, 1369 (1999).
- [9] V. Spagnolo et al., *IEE Proc., Optoelectron.* **150**, 298 (2003).
- [10] V. Spagnolo et al., *Appl. Phys. Lett.* **78**, 1177 (2001).
- [11] C. Zhu, Y. Zhang, A. Li, and Z. Tian, *J. Appl. Phys.* **100**, 053105 (2006).
- [12] C. A. Evans, V. D. Jovanovic, D. Indjin, Z. Ikonc, and P. Harrison, *IEEE J. Quantum Electron.* **42**, 859 (2006).
- [13] A. Lops, V. Spagnolo, and G. Scamarcio, *J. Appl. Phys.* **100**, 043109 (2006).
- [14] E. T. Swartz and R. O. Pohl, *Rev. Mod. Phys.* **61**, 605 (1989).
- [15] A. Balandin and K. L. Wang, *Phys. Rev. B* **58**, 1544 (1998).
- [16] P. G. Klemens, in: *Solid State Physics*, edited by F. Seitz and D. Turnbull, Vol. 7 (Academic, New York, 1958).
- [17] K. Belay, Z. Etzel, D. G. Onn, and T. R. Anthony, *J. Appl. Phys.* **79**, 8336 (1996).
- [18] R. Berman, *Thermal Conduction in Solids* (Clarendon, Oxford, 1978).
- [19] Y. J. Han and P. G. Klemens, *Phys. Rev. B* **48**, 6033 (1993).
- [20] J. Callaway, *Phys. Rev.* **113**, 1046 (1959).
- [21] B. Abeles, *Phys. Rev.* **131**, 1906 (1963).
- [22] S. T. Huxtable, Ph.D. thesis, University of California, Berkeley (2002).
- [23] C. LaBounty, Ph.D. thesis, University of California, Santa Barbara (2001).
- [24] J. S. Yu, S. Slivken, S. R. Darvish, A. Evans, L. Doris, and M. Razeghi, *Appl. Phys. Lett.* **83**, 2503 (2003).